RSC Advances

PAPER

View Article Online
View Journal | View Issue

Cite this: *RSC Adv.*, 2020, **10**, 32058

Activated carbon and palm oil fuel ash as microwave absorbers for microwave-assisted pyrolysis of oil palm shell waste

Sunisa Chuayjumnong,[a] Seppo Karrila,[b] Saysunee Jumrat[b] and Yutthapong Pianroj *[b]

In this study, the effects of two microwave absorbers (MWAb) or catalysts, namely activated carbon (AC) and palm oil fuel ash (POFA), were investigated in microwave pyrolysis of oil palm shell (OPS). The results show similar trends and ranges of the dielectric properties for both MWAbs when measured using a network analyzer with an open-end probe at 2.45 GHz from room temperature to 100 °C. However, according to the Brunauer–Emmett–Teller (BET) method, AC has a larger specific surface area (SSA) and pore volume than POFA. The higher SSA of the AC allows more molecules of gas or liquid substances to be attached on its surfaces than on POFA. This adsorption does not change the structure of AC or POFA. Therefore, on using AC the phenol content was higher than with POFA, as observed from GC-MS peak areas. Both MWAbs had absorbed liquid or gas molecules that may adhere to the surfaces either physically or chemically (or by both types of mechanisms) facilitating bonding to form different molecules. However, phenol derivatives, overall chemical compositions, and product yields were similar for these two MWAbs, according to ANOVA.

Received 5th June 2020
Accepted 24th August 2020

DOI: 10.1039/d0ra04966b

rsc.li/rsc-advances

1. Introduction

Availability of energy is essential to the standard of living and to industrial production, contributing to economy and societal stability. However, many countries lack their own resources for energy production, and look for novel renewable alternatives for energy security and sustainability. In Thailand, the industrial and transportation sectors consume large amounts of fossil fuels, and in 2010 about 80% of the electricity in Thailand was produced from fossil fuels.[1] By investing in alternative energy sources, Thailand seeks to reduce CO_2 emissions by 123 metric tons per year of carbon dioxide equivalent ($MtCO_2$) and improve its domestic energy reserves.[2] In Thailand, the main candidate source for sustainable energy production is biomass. The biomass can include various agricultural waste streams from bagasse, rice husk and straw *etc.* Using biomass to produce energy can reduce greenhouse gas emissions and balance the growth of that biomass. Palm oil production related biomass can include tree trunks, oil palm fiber (OPF), or oil palm shell (OPS), which are by-products from an industry producing several million tons of palm oil per year. Oil palm plantations are distributed throughout Thailand. However, the southern provinces have the most palm oil plantations because of appropriate geophysical conditions, especially Surat Thani, Krabi and Chumphon provinces in southern Thailand. Palm oil is the second most important crop after rubber as source of income, and for export.[3] Usually, this biomass is used as a boiler fuel to produce heat or electricity, producing a large amount of palm oil fuel ash (POFA) waste: approximately 10 million tons per year in Malaysia[4] and 104 tons per year in Thailand.[5] Recently, POFA has been demonstrated as a nourishing fertilizer for gardening, and as a filler in concrete.[5–8]

The conversion of biomass to energy can be done in many ways, including by combustion, gasification, fermentation, and pyrolysis. In laboratory studies microwaving (MW) has been tested for pyrolysis, because it can provide consistently high heating rates while allowing precise control of pyrolysis duration, which affects the quality of the pyrolysis products. Mushtaq *et al.*[9] studied the pyrolysis of OPS with added activated carbon (AC) and showed that the bio-oil contains phenols and 1,1-dimethylhydrazine. The use of AC as MW absorber with biomass in the pyrolysis system helped improve product composition and quantity *via* the improved heating. Salema *et al.*[10] studied pyrolysis with MW energy of OPS and OPF with AC as microwave absorber (MWAb), finding as advantages rapid heat generation, reduced energy consumption, and reduced time and cost. The bio-oil consists of organic compounds, mostly phenolic chemicals. There is also a lot of water along with the organic compounds. Phenols can be high-value

[a]*Major in Energy Technology, Department of Mechanical Engineering, Faculty of Engineering, Prince of Songkla University Hatyai Campus, 15 Karnjanavanich Road, Hat-Yai, Songkhla, 90110, Thailand*

[b]*Faculty of Science and Industrial Technology, Prince of Songkla University Suratthani Campus, 31 Moo 6, Makhamtia, Muang, Suratthani, 84000, Thailand. E-mail: yutthapong.p@psu.ac.th; saysunee.j@psu.ac.th*

chemical precursors of synthetic bioplastics, such as formaldehyde resin or epoxy materials. Phenols are expensive chemicals that can be produced from biomass with high lignin content, so the raw materials are low priced and available in large volumes. The disadvantage of this type of pyrolysis products is uncertain quality with tendency to change during storage. As the liquid from the pyrolysis process contains a wide variety of organic substances, each of which has different chemical properties, storage may result in changes in the properties of those chemicals. The catalyst can improve the yield and favor some compounds in the product, but cannot enable full control of the quality (the proportions of chemicals in bio-oil) that also depends on the type of biomass and pyrolysis conditions. This motivates research and development to improve the stability of bio-oils from MW pyrolysis by using catalysts (MWAb).

The ability of a material to absorb MW energy is determined by its dielectric properties, namely dielectric constant (ε'), dielectric loss factor (ε'') and loss tangent (tan δ).[11] MW heating is based on the interactions between charged particles in a material and the electric field of MW, and also the magnetic field may interact with magnetic dipoles. These mechanisms cause displacements of charges from their average equilibrium positions, which is called polarization. Polarization can be classified into four types. The first is electronic or optical polarization by displacement of electrons from the nuclei. The second is atomic or ionic polarization by displacement of atomic nuclei. The third is dipolar or orientational polarization by rotation of molecules that have permanent dipoles; and the final one is interfacial polarization by the accumulation of relatively mobile charges at grain/phase boundaries or surfaces. In the case of MW, the electric field changes continuously and rapidly with time, so polarization has a phase lag behind that of the electric field because a material's polarization cannot change immediately with the applied field. Thus, the permittivity or the dielectric constant (ε) is expressed by a complex dielectric constant (ε^*) that has both magnitude and phase angle as follows.

$$\varepsilon^* = \varepsilon' - \mathrm{i}\varepsilon'' \quad (1)$$

Here, ε' is the real part of the complex dielectric constant, named dielectric constant. It indicates the ability of the material to store energy. The ε'' is the imaginary part of the complex dielectric constant, named dielectric loss factor, and indicates energy dissipation as heat. The phase angle of the complex number is named loss tangent (tan δ) and is a characteristic of the energy loss in the dielectric material while absorbing MW energy.[10] The angle δ represents the phase lag between the polarization of the material and the applied field. Finally, tan δ is related to ε' and ε'' [according to eqn (2)]. The theory is available in relevant literature.[12–14]

$$\tan\delta = \frac{\varepsilon''}{\varepsilon'} \quad (2)$$

The dielectric electrical properties of a material depend on electric polarity of the molecules. The ability of a dielectric material to convert electromagnetic energy into heat is indicated by the loss tangent.[11] Water has a dielectric constant of 78.5. Salema *et al.*[15] studied the dielectric properties of the agricultural biomass OPS, empty fruit bunch, rice husk, coconut shell and sawdust from room temperature to ~700 °C and at different frequencies. It was found that dielectric properties decreased from 24 to 200 °C due to moisture removal, then decreased from 200 to 450 °C due to decomposition of biomass components and release of volatile matter, and at a temperature of 450 °C found that the dielectric properties increased greatly. Palm oil biomass has a low dielectric constant, so it has a low absorption of MW and it is necessary to add materials that help absorb MW and act as catalysts of pyrolysis. There are many studies on MW pyrolysis of many types of biomass with various MWAb. Undri *et al.*[16] studied pyrolysis of wood pellets in a MW oven with various MWAb choices (No, iron, and carbon). That study found that the pyrolysis of wood pellets is possible with MW without any MWAb, but the conversion will be incomplete. If iron is selected for the MWAb, the coupling reactions will increase the yield of solids and affect the properties of solids and bio-oil. An MWAb should be cheap with consistent properties and good performance. In addition, the ratio of biomass per catalyst must be optimized for maximum performance. The catalyst is used to adjust and improve the quality of bio-oil from pyrolysis of biomass.

This study aimed to test POFA as a MWAb and catalyst with comparison to AC in a MW pyrolysis setup, with a household microwave oven modified by installing the temperature controller with a solid-state relay (SSR) to control sample temperature in the pyrolysis reactor. The production yield of bio-oil and its chemical composition from MW pyrolysis was assessed with varied mixing ratios of OPS and MWAbs, at different pyrolysis temperatures, and the main chemical components were phenols and their derivatives.

2. Materials and methods

2.1 Materials

Oil palm shell (OPS) biomass was provided by the Green Glory Co., Ltd., Tha-Chang, Surat-Thani Province, Thailand. It was ground to 1.18 (ref. 17)–2.00 mm (ref. 18) particle size, and dehydrated in a hot air oven at 105 °C to reduce the moisture content to approximately 8.5% wet basis.[17] The materials for pyrolysis need controlled moisture or water amount that during pyrolysis results in steam reforming. Also, a high moisture content in the material encourages steam gasification. The conversion of biomass from solid into a gas, when heated in a medium of steam, decreases the yield of liquid products. Besides, the liquid product from pyrolysis may contain too much water if the feedstock moisture is not controlled. The dried biomass was stored in zip-lock plastic bags. Normally, biomass with a low moisture content is a poor absorber of microwave (MW) power, so an MW absorber was added (MWAb). It absorbs microwaves and converts the power into heat. Commercial-grade water treatment activated carbon (AC), based on coconut shell, was used as the microwave absorber (MWAb) or the catalyst in previous studies, but here the palm oil

fuel ash (POFA) was tested as an alternative MWAb. Dehydration was done to the two MWAbs. First, their particle size was reduced by grinding to 850 μm, then they were dried in a hot air oven at 105 °C to 8.50% moisture on wet basis. Finally, they were stored in zip-lock plastic bags to maintain the moisture level. Samples of both MWAbs were sent to the Scientific

(a)

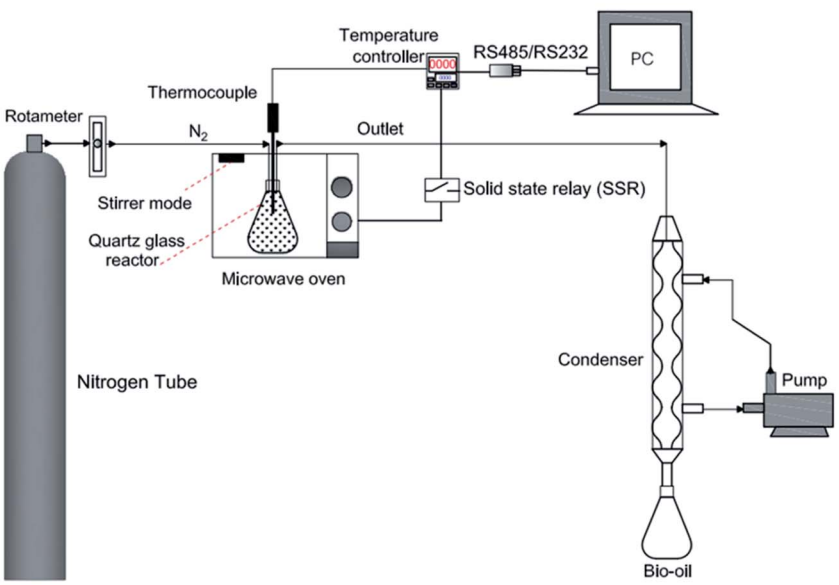

(b)

Fig. 1 Photo (a) and schematic (b) of the experimental microwave pyrolysis system.

Equipment Center, Prince of Songkla University, Hatyai Campus, for proximate analysis (Thermogravimetric Analyzer, TGA7, PerkinElmer, USA), for ultimate analysis (CHNS-O Analyzer, CE Instrument Flash EA1112 Series, Thermo Quest, Italy), and for surface area and porosity analysis by static volumetric N_2 gas adsorption with the Brunauer–Emmett–Teller method (BET: ASAP2460, Micromeritics, USA).

2.2 Experimental set-up

These experiments were carried out in a domestic multimode MW oven with 800 watt maximum power output and 2.45 GHz MW frequency. The pyrolysis reactor was made of quartz with a modified Teflon cap. That cap had three ports: inlet for N_2 flushing, a thermocouple port, and the bio-gas outlet port to the condenser. The temperature feedback control system had a type-K thermocouple providing an analog signal to the temperature controller SHMAX model MAC3D-MSF-EN-NRN. This was the command unit controlling the solid-state relay (SSR). This SSR functioned as an ON–OFF switch of the electric MW power supply. The temperature controller also communicated with a personal computer (PC) by RS485 to RS232 for collecting temperature data. The thermocouple was inserted into the sample from the top of the reactor. A metallic propeller driven at 50 rpm was used to disturb the MW electric field[19] to avoid hot spots in the MW chamber. It improved the heating uniformity inside the MW cavity. Fused quartz container was used as the pyrolysis reactor inside the MW cavity. The condenser collecting vapors into bio-oil form was made of borosilicate glass. It used water at about 6–8 °C as the coolant. This experimental set-up is shown schematically in Fig. 1.

2.3 Method

In each experimental run, 100 g of material was used as this gave appropriate loading level in the reactor. The sample was a mixture of the biomass with the MWAb, with the biomass : MWAb ratio set at 70 : 30, 80 : 20, or 90 : 10. The microwave power was set to 800 W. The atmosphere was flushed out with inert N_2 at a flow rate of 4 LPM[9] for 2 minutes before starting each experiment. In previous studies,[17] it was found that the use of 4 LPM flow rate of N_2 resulted in the most bio-oil (36.75% yield). The inert gas can also play an important role in ensuring safety during the experiment, as it helps avoid an explosions or other dangers from the accumulation of volatile components.[10] The reactor was loaded into the MW cavity and heated for 35 minutes after setting the target temperature to 400, 500, or 600 °C.[20] The reaction time of volatile substances is usually in the range of 5–30 minutes since the components in the volatile phase can react with other components causing the liquid products to increase. The temperature range 400–600 °C causes thermal disintegration and decomposition of the lignocellulose components (cellulose, hemicellulose, and lignin) in the biomass and releases chemicals. The vapors released from the reactor were condensed using a distillation unit to obtain the bio-oil. The condenser was cooled by water at about 6–8 °C. At the end of each experiment, bio-oil and solid phase outputs were measured using a digital scale. The biogas yield was calculated. All the experiments were repeated three times and averages are reported.

After the MW pyrolysis, the products were weighted and the yields were recorded. The three products from MW pyrolysis are in solid, liquid and gas forms. Biochar and MWAb from MW pyrolysis were separated by sieving. The POFA was characterized by Brunauer–Emmett–Teller (BET) analysis, determining surface area and porosity. Also, the heat generation ability when heated by microwave energy was tested for both absorbent materials. Both MWAbs were tested in 100 g amounts, with N_2 flushing of the system to prevent fires with flow rate of 4 LPM. After that, microwave heating was done for 35 minutes to see the temperature of MWAb of each type. The experiment was performed 3 times for each MWAb type and the averages were graphed to see differences in heat generation. The POFA can be used as an MWAb and as a catalyst, based on comparing it to AC. The catalyst substances or objects affect the rates of chemical reactions by changing the activation energy required for a reaction, or the rate of reaction. The MWAb are substances or materials capable of responding to an electromagnetic field and converting it to heat. Each material has different properties and response characteristics in the electromagnetic field, resulting in different heat generation performance. The bio-oil was analysed using a Gas Chromatograph (5977B) – Mass Spectrometer (Triple Quadrupole 7000D model), Agilent, USA, in Gas Chromatography-Electron Ionization/Mass Spectrometer (GC-EI/MS) mode, for chemical composition. GC/MS (Gas Chromatograph/Mass Spectrometer) can resolve the components in a substance by comparing the fingerprints in the mass spectrum for the sample with information in a library (or a database) of known compounds. For GC-MS testing, 1 mL bio-oil sample was extracted with CH_2Cl_2 (1 mL) and vortexed for 1 minute. Then it was diluted with H_2O : Na_2SO_4 in a 10 : 1 ratio and mixed with CH_2Cl_2, and this was filtered through an 0.2-micron nylon membrane before running through the GC-MS. The GC separated volatile organic compounds at an elevated temperature, based on the different preferences of the components between two phases, namely the stationary phase and the mobile phase. Here, on using normal injection mode, the inlet penetration depth was 45 mm, inlet penetration speed 100 mm s^{-1}, and injection flow rate was 100 μL s^{-1}. Run time of GC was 82 min with initial temperature in oven at 70 °C and raised to 250 °C at 2.5 °C min^{-1}, and using the split mode of injector liner Agilent 19 251–60 540 of 990 μL. This analysis uses Agilent CP9205, GC column VF-WAXms 30 × 0.25 (0.25), inner diameter 0.25 mm, length 30 m and film 0.25 microns. As for the MS, it acts as a detector used to measure the compounds contained in the sample. The principle of operation is such that fragments of molecules from the sample are measured for mass and charge, and the relative proportions of these fragment amounts are compared to the reference database for "fingerprints" that represent known compounds. The biogas yield was calculated as follows.

$$\%\ \text{yield of gas} = 100 - (\%\ \text{yield of liquid} + \%\ \text{yield of solid}) \quad (3)$$

2.4 Microwave heating mechanisms and dielectric properties of the materials

In this study, an ENA Series Vector Network Analyzer (VNA); Keysight model E5071C (9 kHz to 8.5 GHz), was used with the coaxial probe to measure the dielectric properties of OPS and MWAbs. The materials were prepared as described in Section 2.1 and were ready in the zip-lock bags for determinations of the dielectric properties. Each powder sample was put in a cylinder and compressed so that the flat surfaces were no longer rough, but were suitable for contact with the probe. The MW frequency 2.45 GHz was used for measurement because this is the operating frequency of the magnetron generating the MW radiation. Before the measurement, a calibration had to be done by connecting the coaxial probe to the VNA with 85070E software, by measuring air, a conductive elastomer short disk, and water. Then, dielectric measurements as functions of material temperature were performed on a hot plate, at 27 (room temperature), 35, 45, 55, 65, and 75 °C. The surface of the material was firmly pressed with the probe head that was held stationary for about 30 seconds to measure the dielectric properties, repeatedly for 5 times, and the means of relative permittivity (ε_r'), relative dielectric loss factor (ε_r''), and loss tangent (tan δ) were recorded.

3. Results and discussion

3.1 Dielectric properties

The dielectric properties as functions of temperature are depicted in Fig. 2. The trends for dielectric constant (ε'), dielectric loss factor (ε''), and tan δ were similar in top, middle and bottom panels. The dielectric properties measured at 2.45 GHz increased with temperature rising from 30 °C but tended to decrease when the temperature was 75 °C. As previously reported,[21] it was found that the dielectric properties will decrease as the temperature increases. In the top panel, the average dielectric constants of OPS, POFA, and AC are 1.44 ± 0.11, 3.39 ± 0.63, and 5.49 ± 1.04, respectively. In the middle panel, the average dielectric loss factors of OPS, POFA, and AC are 0.23 ± 0.05, 0.76 ± 0.27, and 1.67 ± 0.57, respectively. Finally, the bottom panel shows the average tan δ as 0.15, 0.22, and 0.29, for OPS, POFA, and AC, respectively. Our results display similar magnitudes and trends in dielectric properties as those in earlier reports.[21–23] The dielectric properties increased in the rank order OPS, POFA, and AC. Because the OPS is biomass with a low moisture content, it had the lowest dielectric properties. However, AC and POFA used as catalysts and MWAb had activated carbon (AC) solids with few or none of freely rotating dipoles. It has charged particles which can move freely, so electric conduction is possible by the moving charged particles. The collisions of these particles generates heat inside the material. This phenomenon is called Joule heating. The microwave heating of carbon-based solid materials is based on interfacial polarization, called Maxwell–Wagner–Sillars (MWS) polarization.[24] POFA is powdered and contains mostly metal oxides, which have magnetic properties and therefore can respond to the electromagnetic field to produce heat. This heat generation can occur when the size of the material is close to the skin depth of that material.[25] The results of the proximate and

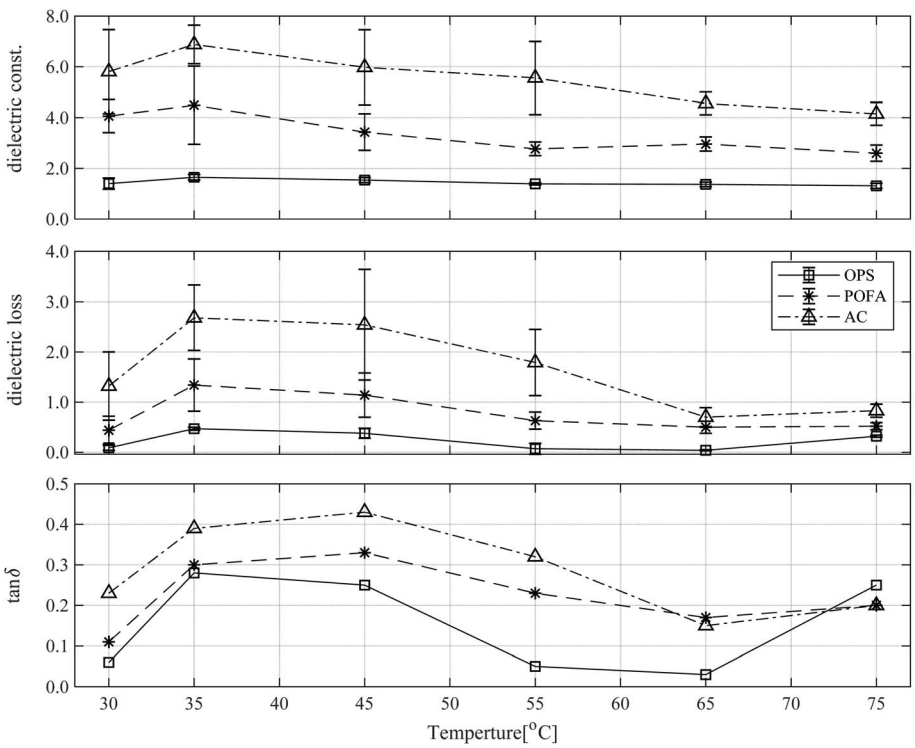

Fig. 2 The VNA measurement results of dielectric properties as functions of temperature: the dielectric constant (ε', top panel), the dielectric loss (ε'', middle panel), and the loss tangent (tan δ, bottom panel).

Table 1 Proximate, ultimate and BET analysis of OPS, AC, and POFA

Parameter	OPS[26]	AC	POFA
Moisture content (wt%)	11.39	8.88 ± 0.04	5.23 ± 0.27
Volatile matter (wt%)	65.76	8.22 ± 0.27	6.53 ± 0.29
Fixed carbon (wt%)	19.73	71.50 ± 0.26	11.76 ± 1.32
Ash (wt%)	3.117	2.40 ± 0.04	78.48 ± 1.87
Carbon (C) (wt%)	45.65 ± 0.26	75.994 ± 0.184	17.418 ± 0.226
Hydrogen (H) (wt%)	5.49 ± 0.06	1.884 ± 0.030	0.413 ± 0.007
Nitrogen (N) (wt%)	0.32 ± 0.01	0.129 ± 0.005	0.160 ± 0.004
Sulfur (S) (wt%)	Not detected	<0.01	0.295 ± 0.003
Oxygen (O) (wt%)	36.59 ± 0.36	14.604 ± 0.119	4.391 ± 0.018
Net heating value (N. H. V.) (kcal kg^{-1})	—	6155.114 ± 10.295	1367.631 ± 16.823
BET surface area (m^2 g^{-1})	—	686	76
Total pore volume (cm^3 g^{-1})	—	0.29	0.04
Average pore diameter (Å)	—	17	23

Table 2 Top eight chemical components in POFA, as analyzed by X-ray fluorescence spectrometry (XRF)

No.	Component	Fraction of total mass (%)
1	Silicon dioxide (SiO_2)	51.2
2	Calcium oxide (CaO)	8.1
3	Potassium oxide (K_2O)	7.2
4	Phosphorus pentoxide (P_2O_5)	4.1
5	Magnesium oxide (MgO)	3.3
6	Aluminum oxide (Al_2O_3)	2.1
7	Sulfur trioxide (SO_3)	1.5
8	Ferric oxide (Fe_2O_3)	1.5

ultimate analysis are summarized in Table 1 (the OPS results came from Pianroj *et al.*[26]).

Moreover, the composition of POFA in this study was characterized by XRF (X-ray fluorescence spectrometer, Zetium, PANalytical, Netherlands), with the top eight chemical components of POFA shown in Table 2. As seen in Table 2, all main components of POFA are oxides and the main component is SiO_2 or silica, which varies from 45–65%.[15–17] Typically, silica is an amorphous colorless solid, and it is extensively used in the dielectric layers that isolate different layers of an integrated circuit (IC). It is used to fabricate dielectric films for capacitors and metal-oxide-semiconductor (MOS) transistors.[18] Crystals could form with chemical or ionic bonds. In the presence of an electric field, electronic polarization and atomic polarization are the two dominant types that play important roles in silica and oxide compounds, while dipolar polarization is usually not present in silica, oxides or silicate compounds.[27]

The temperature evolution of both pure MWAbs, namely AC and POFA, is seen in Fig. 3. In the transient period up to around 15 minutes, both MWAbs have a steep graph. Especially in the first 5 minutes the response of AC is steeper than that of POFA, because the space charges or electrons causing interfacial polarization of AC respond quickly to the MW electric field, more so than the distortion of the symmetrical electron charge distribution (dipole moment) as electron polarization and the displacement of atomic nuclei as atomic polarization. After 15 minutes to the end of the experiment, the temperatures were steady with POFA around 870 °C and with AC around 750 °C. The difference in final temperatures comes from the two polarization types in POFA, which together support stronger MW absorption. In a previous study,[28] microwaves at 2.45 GHz were used to sinter rice husk ash, which is mainly SiO_2 (90.6%) along with other oxides (9.4%). The time profile of temperature and its magnitude are similar as in the current experiments.

3.2 Specific surface area (SSA)

As a widely used standard procedure, the BET method was used to analyze the physisorption of gas by the powder form solids. The nitrogen (N_2) gas adsorption isotherms of POFA and AC, used as catalysts and MWAb, are shown in Fig. 4. The characteristic patterns of adsorption–desorption are similar, both representing Type I isotherms according to International Union of Pure and Applied Chemistry (IUPAC).[29] This type of isotherm is concave in the relative pressure (p/p_0) and the surface excess amount of substance in the adsorbed layer approaches a limit as $p/p_0 \rightarrow 1.0$. Type I isotherms are typical for microporous

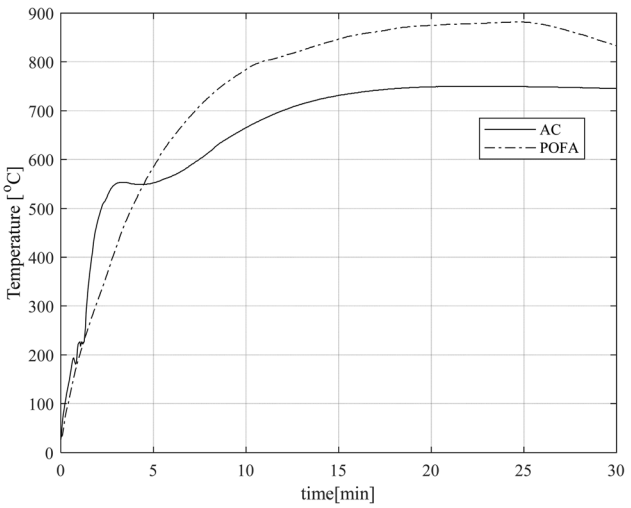

Fig. 3 Time profiles of temperature for the pure MW absorbers (MWAbs) AC and POFA.

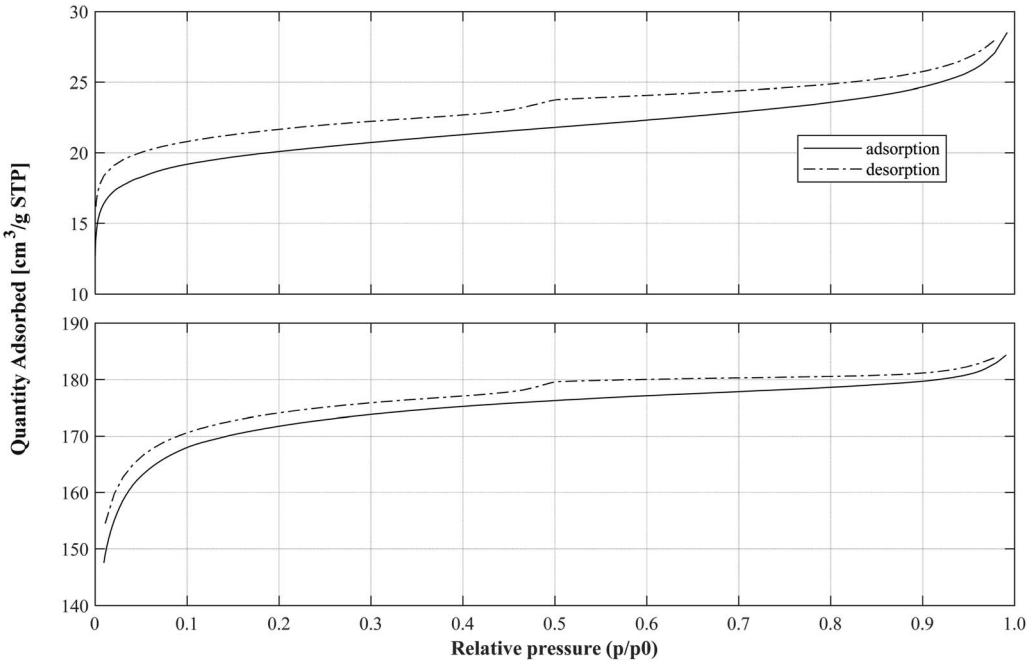

Fig. 4 N_2 adsorption–desorption isotherms of POFA (top panel) and AC (bottom panel).

solids with relatively small external surfaces. In the low relative pressure region with $p/p_0 < 0.1$, the adsorbed volume increases steeply as N_2 was adsorbed mainly in the microporous structure.[30,31] However, while the adsorption–desorption responses of POFA and AC are similar in pattern, the volume adsorbed by AC is about nine-fold greater than that for POFA.

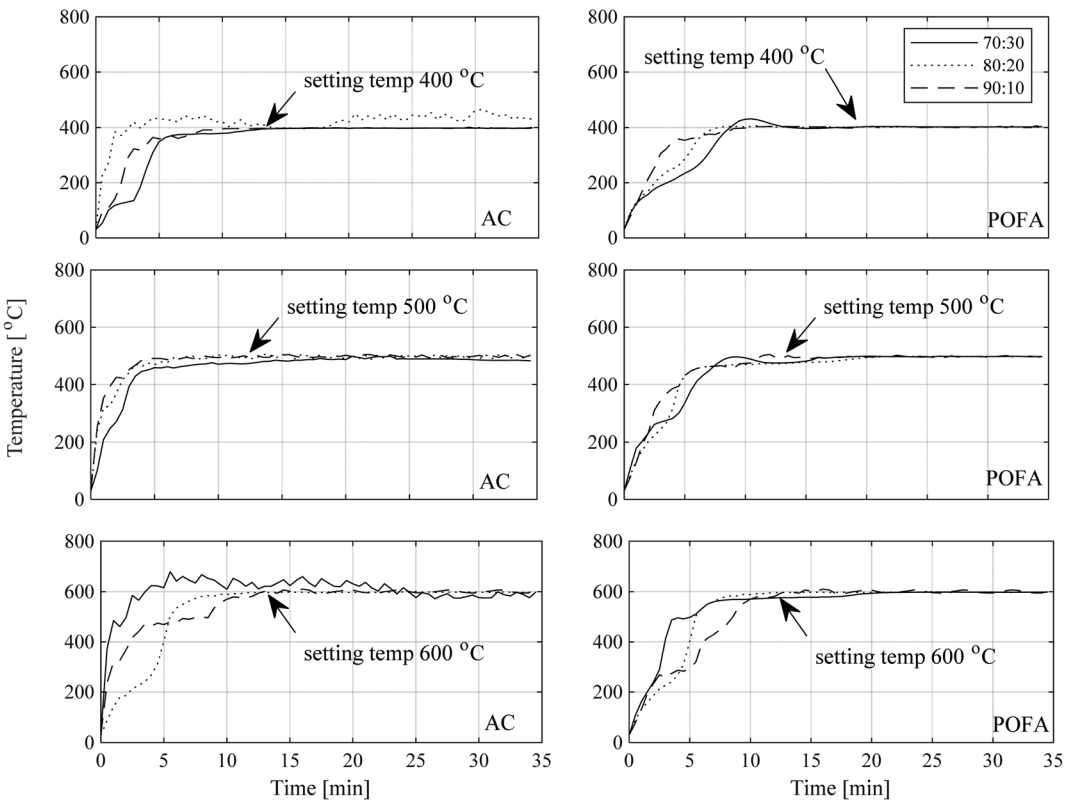

Fig. 5 Temperature profiles during microwave heating. The left column is for AC while the right side is for POFA. The rows from top to bottom are for temperature setpoints 400, 500, and 600 °C, respectively.

This means that AC had larger SSA and pore volume than POFA, see Table 1.

3.3 Temperature profiles

As described in Section 2.3, the blend ratios OPS:AC and OPS:POFA were varied in the batch experiments, each using a total of 100 g blend. The maximal 800 W power of the MW oven was used, and the temperature target was set at 400, 500, or 600 °C and controlled by the temperature controller as explained in Section 2.2. The purpose of these experiments was to assess how the temperature affects the composition of the bio-oil. The results were plotted as functions of MW exposure time, shown in Fig. 5. Every experimental run achieved its temperature target, but mixtures with AC reached that target faster than mixtures with POFA. This is obvious from the steeper slopes in the graphs. From Fig. 5, the biomass to MWAb ratio affects temperature profile at 400 and 500 °C temperatures, and blends with a small amount of biomass tends to have less steep responses. So, around 400 and 500 °C a blend with a small fraction of biomass produces heat more slowly than a blend with more biomass. On the other hand, at 600 °C a blend with less biomass had a greater slope than with a greater amount of biomass. The reason is the fast response of space charges, which react to the electric field of MW as interfacial polarization; this converts MW power into heat effectively as discussed earlier. Factors that affect the thermal characteristics include the shape of the MW reactor, shape and size of the biomass sample, and dielectric properties and heating rate.[32] The temperature will have a slight variance and will gradually stabilize at the desired constant temperature, with support from the MWAb. In addition, dielectric properties of the biomass sample vary with temperature because the lignin in the material decomposes into bio-char and volatile matter.[32] The products and components in the process depend on the MW pyrolysis temperature, and the absorption efficiency of the MWAb as well.

3.4 Product yields

Bio-char, bio-oil, and syngas are the three main products from the pyrolysis, in solid, liquid, and gas phase, respectively. Fig. 6 shows the average product yields (%) of MW pyrolysis across the various MWAb, temperature, and mixture ratio choices tested. The error bars show standard deviations for each experimental condition, estimated from three replications. However, the focus of this study was to maximize the yield of bio-oil, although this may be specific to the run procedures and apparatus used. In this figure, the yield of bio-oil from OPS with AC as the MWAb was in the range 26–38%. For OPS mixed with POFA the bio-oil yield ranged within 22–33%. The highest 38% bio-oil yield was obtained at 500 °C with OPS:AC ratio 70 : 30. Similar conditions for the highest bio-oil yield were found in a previous study by Omoriyekomwan *et al.*[20] The reason why fast pyrolysis can produce a lot of liquid is that fast pyrolysis occurs at 400–600 °C temperatures. The molecules of biomass break down to smaller molecules, and this converts the raw materials from solid-state by sublimation into steam and oil and gas, collected by condensation into liquid. The dominant product type from this process is liquid, which is different from slow pyrolysis at less than 450 °C.

One-way analysis of variance (ANOVA) was run in MS-Excel (with the analysis toolpak add-in) to determine whether all group means were similar without statistically significant differences. The statistical confidence level was set at 95%, so that p-value < 0.05 was required to reject the null hypothesis (H_0). Firstly, to determine the effects of pyrolysis temperature for each MWAb at a fixed mixture ratio, H_0: the mean product yield of bio-oil is the same for each pyrolysis temperature; and H_1: the mean product yields of bio-oil are not the same. The results are shown in Table 3. Most p-values are greater than 0.05 favoring the null hypothesis. This indicates that the pyrolysis temperatures 400, 500, and 600 °C did not significantly affect the mean yield of bio-oil at a fixed mixture ratio with either MWAb. Next the effects of different mixture ratios were tested for each MWAb by fixed pyrolysis temperature. In this case, the

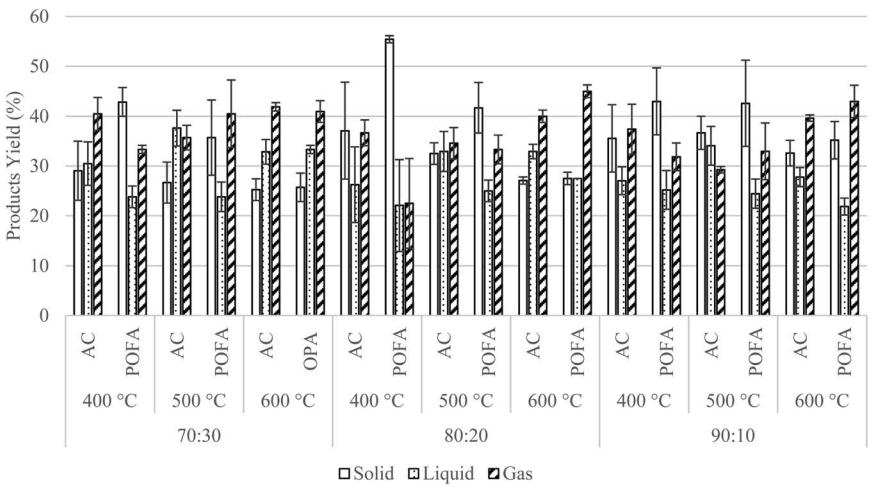

Fig. 6 The average product yields (%) from MW pyrolysis, shown by choice of MWAb, temperature, and mixture ratio.

Table 3 The p-values from one-way ANOVA for checking effects of pyrolysis temperature and mixture ratio

	Effect of pyrolysis temperature at fixed mixture ratio (OPS : MWAb)			Effect of mixture ratio at each pyrolysis temperature level		
MWAbs	70 : 30	80 : 20	90 : 10	400 °C	500 °C	600 °C
AC	0.10	0.25	0.05	0.61	0.36	0.00
POFA	0.01	0.52	0.41	0.82	0.87	0.00

Table 4 The p-values from one-way ANOVA for difference between AC and POFA when used as MWAb

	Mixture ratio (OPS : MWAb)		
Temperature	70 : 30	80 : 20	90 : 10
400 °C	0.08	0.58	0.54
500 °C	0.01	0.04	0.03
600 °C	0.02	0.00	0.02

hypotheses were H_0: the mean product yield of bio-oil is the same for each mixture ratio; and H_1: the mean product yields of bio-oil are not the same. The p-values are shown in Table 3, indicating acceptance of the null hypothesis at pyrolysis temperatures 400 and 500 °C for both MWAbs: the mean yields of bio-oil were similar for each mixture ratio at these two temperature levels. However, with the pyrolysis temperature at 600 °C both MWAbs show $p < 0.05$, so the null hypothesis is rejected and alternative hypothesis is accepted: the mixture ratios differed, because at this high a temperature MW pyrolysis favored the formation of non-condensable gases. This is consistent with results reported in ref. 33.

Finally, we assess the effect of the alternative MWAb types AC and POFA, when the pyrolysis temperature and the mixing ratio are fixed. The hypotheses are H_0: the mean product yield of bio-oil is the same for each MWAb; and H_1: the mean product yields of bio-oil are not the same. The p-values from one-way ANOVA are shown in Table 4. The mean product yields of bio-oil were similar with p-values greater than 0.05, except for the high 500 and 600 °C temperatures with $p < 0.05$. Therefore, the type of MWAb did not affect bio-oil yield at comparatively low temperatures, but did at the highest tested temperatures. The liquid products offer significant advantages to the fast pyrolysis.[34,35]

3.5 Characterization of bio-oil by GC-MS

Bio-oil samples from microwave pyrolysis experiments with various mixture ratios at various temperatures were characterized by GC-MS analysis. The averages and standard deviations (taken across all experiments) are compared between AC and POFA in Table 5. It was found that the main chemical components were phenol derivatives and organic acids. Moreover, the highest phenol concentration was obtained by using AC as a microwave absorber instead of POFA. The mechanisms of phenol formation affected by MWAb type used in microwave pyrolysis are discussed in ref. 20 and 36. The AC has a larger specific surface and porosity (volume fraction of pores) than POFA. These were analyzed with a BET apparatus, with the results shown in Table 1. The results indicate larger SSA and pore volume for AC, which enhanced its catalytic activity the selectively favored phenols in the bio-oil. Both MWAbs had absorbed liquid or gas molecules, which may adhere to the surface either physically or chemically or by both mechanisms, causing bonding or coagulation into different molecules. The proportions of chemical components in the bio-oil vary depending on factors such as surface area and pore structure,

Table 5 The averages and standard deviations of the main chemical compounds (% area in GC-MS) identified in bio-oil samples from microwave pyrolysis with AC and POFA[a]

Chemical component	AC	POFA
Organic acid	18.91 ± 5.51	17.92 ± 5.52
Alcohols	2.64 ± 1.43	2.69 ± 0.81
Aldehyde and ketones	9.68 ± 1.55	10.08 ± 2.43
Other compounds	5.44 ± 2.57	5.97 ± 2.75
Phenol derivatives	57.50 ± 4.44	56.17 ± 4.23
Phenol	36.02 ± 2.86	33.95 ± 4.35
Phenol, 2-methoxy-	5.15 ± 0.35	4.66 ± 0.13
Phenol, 2,6-dimethoxy-	5.35 ± 0.65	5.15 ± 0.74
Phenol, 2,6-dimethoxy-4-(2-propenyl)-	0.77 ± 0.16	0.53 ± 0.22
Phenol, 2-methoxy-4-propyl-	0.88 ± 0.00	0.68 ± 0.00
Phenol, 2-methoxy-4-(1-propenyl)-	0.42 ± 0.00	ND
Phenol, 2-methoxy-4-(1-propenyl)-, acetate	0.19 ± 0.00	ND
Phenol, 2-methoxy-4-(1-propenyl)-, (*Z*)-	ND	3.17 ± 0.00
Phenol, 2-methoxy-4-(1-propenyl)-, (*E*)-	ND	1.39 ± 0.00
Phenol, 2-methyl-	ND	0.81 ± 0.00
Phenol, 4-methyl-	1.08 ± 0.04	0.50 ± 0.38
2-Methoxy-4-(*n*-propyl)phenol	0.145 ± 0.01	0.29 ± 0.17
2-Methoxy-4-vinylphenol	0.35 ± 0.22	0.56 ± 0.26
(*E*)-2,6-Dimethoxy-4-(prop-1-en-1-yl)phenol	3.11 ± 0.00	2.61 ± 1.32
3-Allyl-6-methoxyphenol	0.44 ± 0.00	0.37 ± 0.00
2-Ethyl-phenol	0.28 ± 0.00	0.23 ± 0.00
4-Ethylphenol	4.54 ± 6.31	0.17 ± 0.06
m-Ethyl-phenol	0.40 ± 0.11	0.44 ± 0.18
5-*tert*-Butylpyrogallol	2.05 ± 1.45	1.44 ± 0.47
3,5-Dimethoxy-4-hydroxytoluene	2.85 ± 1.43	2.82 ± 1.05
4-Propyl-syringol	0.61 ± 0.61	0.21 ± 0.00
trans-4-Propenyl-syringol	1.29 ± 1.17	0.23 ± 0.18
Creosol	3.02 ± 0.00	3.06 ± 0.48
p-Cresol	1.19 ± 0.16	0.79 ± 0.00
o-Cresol	ND	1.02 ± 0.00
m-Cresol	0.895 ± 0.04	0.95 ± 0.07
Guaiacol, 4-ethyl-	3.38 ± 0.91	2.22 ± 0.46
trans-Isoeugenol	1.14 ± 0.00	1.18 ± 1.09

[a] ND = not detected = concentration below limit of detection.

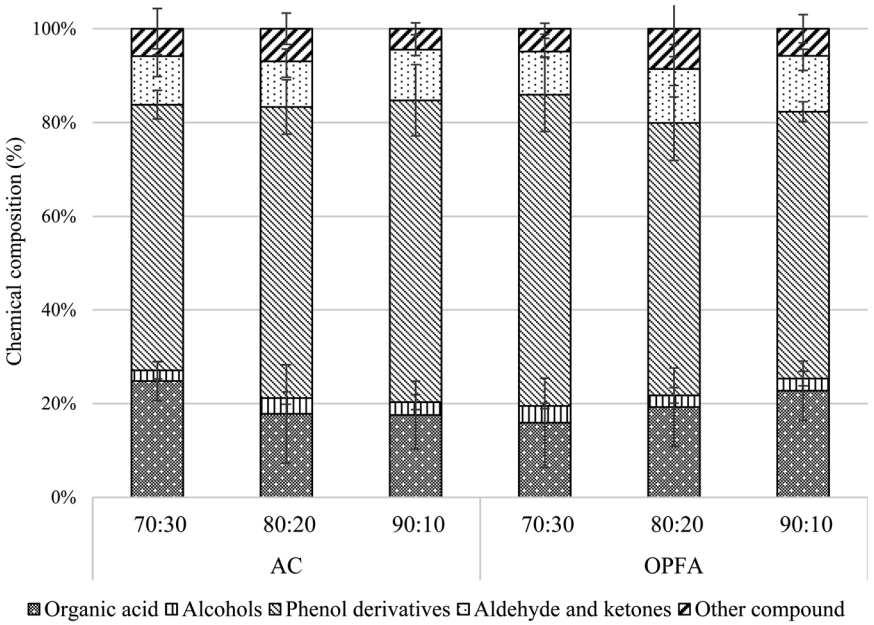

Fig. 7 Chemical composition of liquid products from the MW pyrolysis as determined by GC-MS.

size, functional groups on the surfaces, polarity of molecules, temperature, and turbulence. As the pyrolysis temperature was increased, large chemical molecules tended to be broken down into many smaller molecules, according to the GC-MS results. Moreover, increasing the pyrolysis temperature tends to decrease some phenol contents, as these get broken down to phenol derivatives as shown in Fig. 7. This tendency has been reported earlier.[19,26] The mixture ratio and choice of MWAb did not significantly affect the chemical composition of the bio-oil from MW pyrolysis. The chemical composition of the bio-oil obtained from the pyrolysis process depends on the composition of the starting material and on the process conditions, such as heating rate, temperature, *etc.* Here, the microwaves give a rapid heating rate in the pyrolysis, affecting the proportions of chemical components, which in this study were mostly phenolic chemicals and phenolic derivatives. However, one-way ANOVA comparing the means of phenol derivatives between AC and POFA gave $p = 0.79$, which indicates no statistical significance. The null hypothesis is accepted, rejecting the alternative that there is a difference in the mean of phenol derivatives between AC and POFA. The overall concentration of phenol derivatives is considered similar with AC and POFA.

4. Conclusions

Palm oil fuel ash (POFA) was tested as an alternative microwave absorber or catalyst, and compared to activated carbon (AC) in the pyrolysis of oil palm shell (OPS). The bio-oil yields with AC ranged within 26–38% and with POFA within 22–33%. The highest 38% bio-oil yield was obtained at 500 °C feedback controlled pyrolysis temperature, with OPS:AC blend ratio 70 : 30. The AC and POFA did not significantly differ in bio-oil yield, but AC tends to give more phenol products due to its comparatively high specific surface and porosity. On increasing pyrolysis temperature the number of chemical components produced tends to increase according to GC-MS analysis of the bio-oil. MWAb choice affects the microwave pyrolysis of OPS because it can accelerate heat generation and temperature rise during fast pyrolysis, and can help improve the quality of the liquid product from pyrolysis. Both MWAbs are capable of absorbing microwave energy, accelerating reactions, and extracting phenol compounds from biomass. The choice of MWAb for microwave pyrolysis must consider the basic properties of the material, the ability to absorb microwaves into heat energy, the surface area, and the pore size that affect the adsorption and selection, yield, and proportions of chemical components in the bio-oil. In this study there was an optimal amount of absorbent (in proportion to the main feedstock) that maximized the liquid yield. Mostly that oil was composed of phenolic compounds that are commercially valuable. Improving the quality of the oil is an important issue for cost-effective operation of pyrolysis, and this study supports such optimization.

Conflicts of interest

There are no conflicts to declare.

Acknowledgements

This work was supported by the National Research Council of Thailand under project Research University Network (RUN), Energy: sub-project: 4/2559. We thank Dr Sopida Sangsuntorn, Department of Mechanical Engineering, Faculty of Engineering, Rajamangala University of Technology Rattankosin, Nakhon Pathom province, Thailand, for contribution to dielectric

measurement section, and Miss Sunisa Chuayjumnong thanks the Interdisciplinary Graduate School of Energy System, Prince of Songkla University, for supporting scholarships under contact no. IGS-Energy: 1-2018/10.

References

1 J. Kamsamrong and C. Sorapipatana, *Sustainable Energy Technologies and Assessments*, 2014, **7**, 45–54.
2 J. Martchamadol and S. Kumar, *Renewable Sustainable Energy Rev.*, 2012, **16**, 6103–6122.
3 P. Nutongkaew, J. Waewsak, W. Riansut, C. Kongruang and Y. Gagnon, *Sustainable Energy Technologies and Assessments*, 2019, **35**, 189–203.
4 M. Safiuddin, M. Abdus Salam and M. Zamin Jumaat, *J. Civ. Eng. Manag.*, 2011, **17**, 234–247.
5 E. Khankhaje, M. W. Hussin, J. Mirza, M. Rafieizonooz, M. R. Salim, H. C. Siong and M. N. M. Warid, *Mater. Des.*, 2016, **89**, 385–398.
6 W. Tangchirapat, C. Jaturapitakkul and P. Chindaprasirt, *Constr. Build. Mater.*, 2009, **23**, 2641–2646.
7 H. M. Hamada, G. A. Jokhio, F. M. Yahaya, A. M. Humada and Y. Gul, *Constr. Build. Mater.*, 2018, **175**, 26–40.
8 K. Wi, H.-S. Lee, S. Lim, H. Song, M. W. Hussin and M. A. Ismail, *Constr. Build. Mater.*, 2018, **183**, 139–149.
9 F. Mushtaq, T. A. T. Abdullah, R. Mat and F. N. Ani, *Bioresour. Technol.*, 2015, **190**, 442–450.
10 A. A. Salema and F. N. Ani, *Bioresour. Technol.*, 2011, **102**, 3388–3395.
11 A. A. Salema, Y. K. Yeow, K. Ishaque, F. N. Ani, M. T. Afzal and A. Hassan, *Ind. Crops Prod.*, 2013, **50**, 366–374.
12 A. R. Von Hippel, *Dielectrics and waves*, Artech House, Boston, Mass., 1995.
13 G. G. Raju, *Dielectrics in electric fields*, CRC Press, 6000 Broken Sound Parkway NW, USA, 2017.
14 H. J. Kitchen, S. R. Vallance, J. L. Kennedy, N. Tapia-Ruiz, L. Carassiti, A. Harrison, A. G. Whittaker, T. D. Drysdale, S. W. Kingman and D. H. Gregory, *Chem. Rev.*, 2014, **114**, 1170–1206.
15 A. A. Salema, F. N. Ani, J. Mouris and R. Hutcheon, *Fuel Process. Technol.*, 2017, **166**, 164–173.
16 A. Undri, M. Abou-Zaid, C. Briens, F. Berruti, L. Rosi, M. Bartoli, M. Frediani and P. Frediani, *Fuel*, 2015, **153**, 464–482.
17 F. Mushtaq, T. A. Abdullah, R. Mat and F. N. Ani, *Bioresour. Technol.*, 2015, **190**, 442–450.
18 A. Palamanit, P. Khongphakdi, Y. Tirawanichakul and N. Phusunti, *Biofuel Res. J.*, 2019, **6**, 1065–1079.
19 Z. Abubakar, A. A. Salema and F. N. Ani, *Bioresour. Technol.*, 2013, **128**, 578–585.
20 J. E. Omoriyekomwan, A. Tahmasebi and J. Yu, *Bioresour. Technol.*, 2016, **207**, 188–196.
21 M. Tripathi, J. N. Sahu, P. Ganesan, P. Monash and T. K. Dey, *J. Anal. Appl. Pyrolysis*, 2015, **112**, 306–312.
22 J. A. Menéndez, A. Arenillas, B. Fidalgo, Y. Fernández, L. Zubizarreta, E. G. Calvo and J. M. Bermúdez, *Fuel Process. Technol.*, 2010, **91**, 1–8.
23 J. E. Atwater and R. R. Wheeler, *Appl. Phys. A: Mater. Sci. Process.*, 2004, **79**, 125–129.
24 T. Kim, J. Lee and K.-H. Lee, *Carbon Lett.*, 2014, **15**, 15–24.
25 J. Sun, W. Wang and Q. Yue, *Materials*, 2016, **9**, 231–255.
26 Y. Pianroj, S. Jumrat, W. Werapun, S. Karrila and C. Tongurai, *Chem. Eng. Process.*, 2016, **106**, 42–49.
27 A. C. Lasaga and R. T. Cygan, *Am. Mineral.*, 1982, **67**, 328–334.
28 N. Makul and D. K. Agrawal, *Mater. Lett.*, 2010, **64**, 367–370.
29 K. S. W. Sing, *Journal*, 1985, **57**, 603–619.
30 A. R. Hidayu, N. F. Mohamad, S. Matali and A. S. A. K. Sharifah, *Procedia Eng.*, 2013, **68**, 379–384.
31 K. S. K. Reddy, A. Al Shoaibi and C. Srinivasakannan, *Waste Biomass Valorization*, 2012, **3**, 149–156.
32 S. Gadkari, B. Fidalgo and S. Gu, *Fuel Process. Technol.*, 2017, **156**, 473–484.
33 Q. Bu, H. Lei, S. Ren, L. Wang, Q. Zhang, J. Tang and R. Ruan, *Bioresour. Technol.*, 2012, **108**, 274–279.
34 A. V. Bridgwater and G. V. C. Peacocke, *Renewable Sustainable Energy Rev.*, 2000, **4**, 1–73.
35 A. Dufour, P. Girods, E. Masson, Y. Rogaume and A. Zoulalian, *Int. J. Hydrogen Energy*, 2009, **34**, 1726–1734.
36 Q. Bu, H. Lei, L. Wang, Y. Wei, L. Zhu, Y. Liu, J. Liang and J. Tang, *Bioresour. Technol.*, 2013, **142**, 546–552.

